Research article

Prediction of potential inhibitors of SARS-CoV-2 using 3D-QSAR, molecular docking modeling and ADMET properties

Ayoub Khaldan [a], Soukaina Bouamrane [a], Fatima En-Nahli [a], Reda El-mernissi [a], Khalil El khatabi [a], Rachid Hmamouchi [a], Hamid Maghat [a], Mohammed Aziz Ajana [a], Abdelouahid Sbai [a,*], Mohammed Bouachrine [a,b], Tahar Lakhlifi [a]

[a] Molecular Chemistry and Natural Substances Laboratory, Faculty of Science, Moulay Ismail University of Meknes, Morocco
[b] EST Khenifra, Sultan Moulay Sliman University, Benimellal, Morocco

ARTICLE INFO

ABSTRACT

Coronavirus (COVID-19), an enveloped RNA virus, primarily affects human beings. It has been deemed by the World Health Organization (WHO) as a pandemic. For this reason, COVID-19 has become one of the most lethal viruses which the modern world has ever witnessed although some established pharmaceutical companies allege that they have come up with a remedy for COVID-19. To that end, a set of carboxamides sulfonamide derivatives has been under study using 3D-QSAR approach. CoMFA and CoMSIA are one of the most cardinal techniques used in molecular modeling to mold a worthwhile 3D-QSAR model. The expected predictability has been achieved using the CoMFA model ($Q^2 = 0.579$; $R^2 = 0.989$; $R^2test = 0.791$) and the CoMSIA model ($Q^2 = 0.542$; $R^2 = 0.975$; $R^2test = 0.964$). In a similar vein, the contour maps extracted from both CoMFA and CoMSIA models provide much useful information to determine the structural requirements impacting the activity; subsequently, these contour maps pave the way for proposing 8 compounds with important predicted activities. The molecular surflex-docking simulation has been adopted to scrutinize the interactions existing between potentially and used antimalarial molecule on a large scale, called Chloroquine (CQ) and the proposed carboxamides sulfonamide analogs with COVID-19 main protease (PDB: 6LU7). The outcomes of the molecular docking point out that the new molecule P1 has high stability in the active site of COVID-19 and an efficient binding affinity (total scoring) in relation with the Chloroquine. Last of all, the newly designed carboxamides sulfonamide molecules have been evaluated for their oral bioavailability and toxicity, the results point out that these scaffolds have cardinal ADMET properties and can be granted as reliable inhibitors against COVID-19.

1. Introduction

In December 2019, pneumonia stricken patients of unknown factors were first beheld in Wuhan, China [1]. Later, the epidemic was considered as an unparalleled enveloped RNA beta Coronavirus disease 2019 (COVID-19) [2]. This disease was defined and identified as a Severe Acute Respiratory Syndrome Corona Virus 2 (SARS-CoV-2), which has much in common with SARS-CoV from a phylogenetic perspective [3]. Because of its lethality and outbreak, COVID-19 has been regarded by the WHO as one of the medical challenges to which the whole world is making face [4]. In the eyes of the WHO, the disease precipitated by SARS-CoV-2 is extremely infectious; hence, this virus has gone worldwide, resulting in higher mortality rates. Although there are many symptoms behind COVID-19, they can run as follows: fever, fatigue, dry cough and breathing difficulties. Nonetheless, there are some people who can be prone to the virus without bearing any symptoms [4]. Their immune system could have resisted it.

The eruption of COVID-19 has borne negatively on peoples' daily lives. As a matter of fact, it has threatened their health physically, mentally, and psychologically and hampered social and economic development [5]. People during the period of the quarantine were suffering from a plethora of depressive symptoms due to many reasons among which lack of physical activity and fear are the most common ones. Scientists and researchers are racing to be honored to find vaccines or drugs against COVID-19. Nevertheless, there is no specific drug that has been reported because the production of an efficacious and reliable drug requires a long time of research and clinical trials. Consequently,
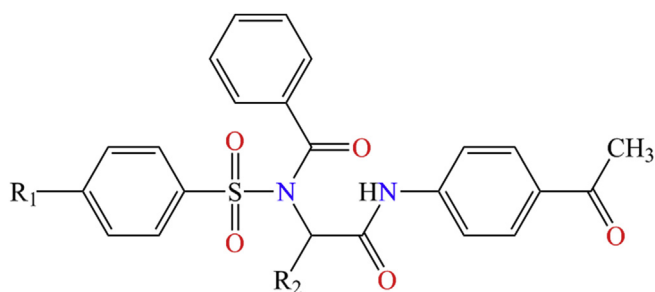

Figure 1. General structure of carboxamides sulfonamide derivatives.

drug repositioning has been a strategy adopted by several researchers to seek effective treatment in a short period of time.

Chloroquine (CQ) is an antimalarial medication developed to substitute natural antimalarial medicines by Bayer in Germany in 1934. This medicine has been adopted to treat COVID-19 affecting patients and reveals desirable results [6,7,8,9]. CQ has much in common with UDP-N-acetylglucosamine 2- epimerase structurally, which prevents or limits quinone reeducates 2, which is an enzyme involved in the biosynthesis of sialic acids [8]. The potential intervention of sialic acid biosynthesis by CQ may be held responsible for this drug's wide antiviral range [8]. Nonetheless, the interactions between COVID-19 and the Chloroquine mechanism is neither clear, nor guaranteed.

Sulfonamides are biologically active compounds since they are of crucial importance. There are many sulphonamide drugs on the markets for treating diseases of different nature [10]. Sulfonamide derivatives, such as methazolamide, dichlorophenamide, ethoxzolamide, acetazolamide, and dorzolamide have been clinically bet on for decades as inhibitors of the zinc enzyme carbonic anhydrase [10]. Because of their affordability and low cost, they are heavily used as veterinary antibiotics in most parts of the world, especially in Asia, some parts of Europe and many rising countries [11]. Sulfonamide derivatives are an important moiety of numerous ranges of bioactive compounds and pharmaceutical molecules like antibacterial [12], anticancer [13,14], anti-inflammatory [15], antitumor [16] and antimalarial [17,18,19].

Three-dimensional quantitative structure-activity relationship (3D-QSAR) is a cardinal method used in molecular modeling and has been relied on to find out new potent molecule in order to cure severe diseases [20]. The main purpose of this method is to associate biological properties with structural descriptors, and is put into practice to predict the activity value of non-synthesized molecules, which are structurally linked to the training sets [21]. The Comparative Molecular Field Analysis (CoMFA) and the Comparative Molecular Similarity Indices Analysis (CoMSIA) are primarily two common techniques used in 3D-QSAR. The rationale behind them is to identify the geometric information required for determining the preferred and non-preferred regions for the biological activity [21].

The techniques of structure-based approaches, including molecular docking, are regarded as one of the most decisive methods in coming up with new potent drugs [22,23]. This technique centers on studying in-depth the interactions existing between the ligand and the receptor so as to scrutinize the binding mechanism between them.

Owing to the public health issue and lack of an effective cure, many countries are opting for the Chloroquine as antimalarial drug for the treatment of COVID-19. Therefore, it has become an urgency to try to discover new drugs that can be more credible and effective without having any harmful side effects than the Chloroquine used to cure the new pandemic. To that end, a set of eighteen carboxamides sulfonamide analogs, covered in literature, present antimalarial activity [24] was studied using both CoMFA [25] and CoMSIA [26] approaches. In addition, molecular docking simulation was achieved to scrutinize the binding mechanism existing between SARS-CoV-2 main protease and carboxamides sulfonamide compounds. Lastly, ADMET (Absorption,

Distribution, Metabolism, Excretion, and Toxicity) properties were conducted in order to assess the oral bioavailability of the newly carboxamides sulfonamide scaffolds and measure their toxicity.

2. Material and methods

2.1. Data set and biological activity

The reliability of the QSAR study relies on the available database, the technique of analysis and the validation tests. In this study, the antimalarial activity and chemical structures of 18 carboxamides sulfonamide derivatives were taken from literature [24]. These molecules were deemed to conduct the 3D-QSAR analysis by splitting the database into two groups; a training set of 14 molecules to develop the quantitative model and a test set of 4 compounds to confirm the proficiency of the molded model. The chemical structures of carboxamides sulfonamide compounds and their values of the activity are clarified in Figure 1 and Table 1. For the calculations, the all experimental MIC (μM) activity values were transformed to the negative logarithm of MIC, (pMIC = $-\log_{10}$ (MIC)).

2.2. Minimization and molecular alignment

Molecular alignment deemed as one of the most cardinal factor in the development of 3D-QSAR models. In this paper, the SYBYL-X 2.0 molecular modeling program was adopted for all modeling analysis. Indeed, all carboxamides sulfonamide derivatives were sketched with sketch module and minimized using the Tripos force field, Gasteiger Huckel charges [27,28], and 0.01 kcal/mol as convergence criteria [29], which are existing in SYBYL software. The 18 carboxamides sulfonamide molecules were aligned on the common core using molecule **9** (The more active molecule in the dataset) as a reference as shown in Figure 2.

2.3. CoMFA and CoMSIA studies

CoMFA and CoMSIA techniques have been conducted based on molecular alignment to inspect the specific contributions of electrostatic, steric, hydrophobic, donor, and acceptor fields. These methods are based on descriptors of 3D-structures, which deal with some of the major shortages underlying classical methods. These descriptors are directly linked to geometry in the space of compounds and to the nature of the atoms that compose them. Potentials are represented by their position and expansion in space as well as their intensity [30].
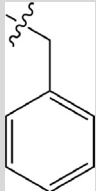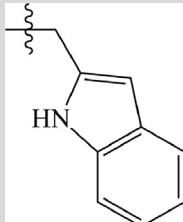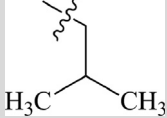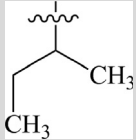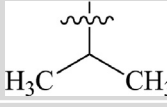
2.3.1. CoMFA studies
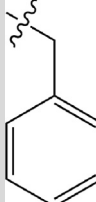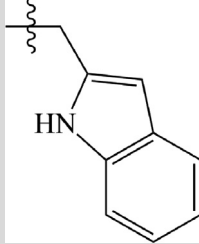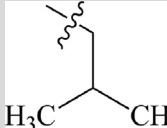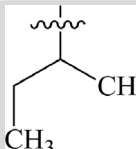
CoMFA study was put into practice in order to analyse the steric and electrostatic effects based on the molecular alignment. To that end, the electrostatic and steric factors were measured using CoMFA technique at each lattice intersection point of a regularly spaced grid of 2.0 Å and based on Lennard Jones and Coulomb potentials. The default value of 30 kcal/mol was limited for energy cutoff calculations [31]. The Partial least squares (PLS) analysis was adopted to establish a linear relationship between the antimalarial activity and the CoMFA and CoMSIA descriptors [32]. The PLS was conducted to provide the coefficient of cross-validation correlation (Q^2) and the optimum number of components (N) using leave-one-out cross-validation. In a similar vein, the non-cross validation analysis was executed to calculate the correlation coefficient (R^2), the standard error of estimate (SEE) and F-test value (F). The cardinal values of Q^2 and R^2 and lower value of SEE were adopted to select the best 3D-QSAR model. The external validation was executed to assay the performance of the proposed model using 4 compounds as a test set.
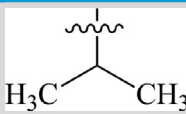
2.3.2. CoMSIA studies
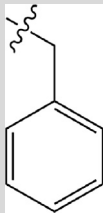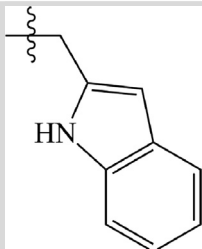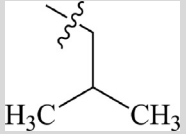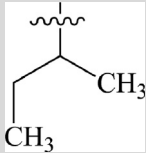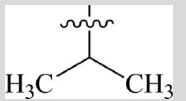
The CoMSIA [26] technique computes the others physico-chemical descriptors, as hydrophobic, hydrogen bond acceptor and hydrogen

Table 1. Experimental pMIC values of 18 carboxamides sulfonamide analogs and their chemical structures.

N°	Structure		MIC (µM)	pMIC
	R₁	R₂		
1	CH₃	H	0.72	6.143
2	CH₃		0.78	6.108
3	CH₃		0.03	7.523
4*	CH₃		0.17	6.770
5	CH₃		5.11	5.292
6	CH₃		2.82	5.550
7	NO₂	H	0.18	6.745
8	NO₂		0.08	7.097
9	NO₂		0.02	7.699
10	NO₂		0.06	7.222
11*	NO₂		0.20	6.699

(continued on next page)

Table 1 (*continued*)

N°	Structure		MIC (μM)	pMIC
	R₁	R₂		
12*	NO₂		1.57	5.804
13	H	H	0.97	6.013
14	H		0.90	6.046
15	H		0.05	7.301
16*	H		0.26	6.585
17	H		1.25	5.903
18	H		1.70	5.770

* Test set molecules.

bond donor fields by the same parameters (Probe atom and lattice box) which are dopted in CoMFA analysis. During the CoMSIA analysis, the minimum sigma (column filtering) was fixed to 2.0 kcal/, and the energy cutoff values was limited to 30 kcal/mol respectively.

2.4. Model performance

Among the goals of this research is to mold a trustworthy 3D-QSAR model with important predictive capability. In this paper, the biological activities of four carboxamides sulfonamide scaffolds were predicted using the suggested 3D-QSAR model in order to evaluate the external predictive capacity of the molded model [33]. These compounds were aligned to the template using the same technique which is adopted in the training set. This validation is marked by the external validation correlation coefficient R^2test.

2.5. Y-randomization test

The construction of a QSAR model is an important step; however, without validation, it remains inadequate that is why the Y-randomization test was applied to test capability of the molded model [34]. To do this, the pMIC values are randomly shuffled and after each shuffle, a 3D-QSAR model was established. The weak values of Q^2 and R^2 hint the

high robustness of QSAR models, whilst the high values of Q^2 and R^2 suggest that these models cannot be considered reliable for this data set owing to the structural redundancy and chance correlation. Therefore, the goal of this technique is to shun any possibility of chance correlation.

2.6. Prediction of the activity of novel compounds

After constructing and validating a QSAR model, it can be opted to predict the activity of the new suggested molecules based on the information of contour maps provided by the molded 3D-QSAR models. According to these initial predictions, the molecules can be modified altogether in the hope of improving their predicted activity. The same procedure was executed with regard to the designed molecules (sketch, convert to 3D structures, minimization, and alignment). Afterwards, the proposed 8 carboxamides sulfonamide scaffolds, along with the training set (14 compounds), were aligned and their inhibitory activities were predicted using the selected 3D- QSAR model; to execute a docking simulation, the one with higher predicted pMIC values was selected.

2.7. Molecular docking simulation

Molecular docking is an important process used in the realm of medicinal chemistry to probe the types and modes of interactions existing
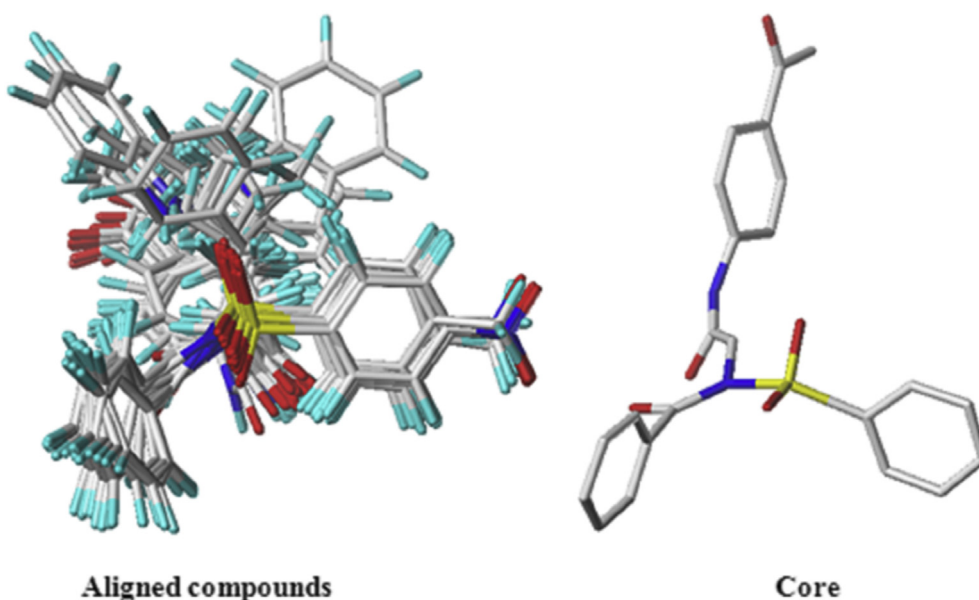
Figure 2. Alignment of 18 carboxamides sulfonamides derivatives using molecule **9** as a template.

Table 2. PLS Statistic indicators of CoMFA and CoMSIA models.

Model	Q2	R^2	SEE	F	N	R^2test	Fractions				
							Ster	Elec	Hyd	Acc	Don
CoMFA	0.579	0.989	0.097	209.678	4	0.791	0.536	0.464	-	-	-
CoMSIA	0.542	0.975	0.148	88.931	4	0.964	0.115	0.321	0.277	0.128	0.159

Q^2: Cross-validated correlation coefficient; R^2: Non-cross-validated correlation coefficient; SEE: Standard error of the estimate.
N: Optimum number of components; F: F-test value; R^2test: External validation correlation coefficient.
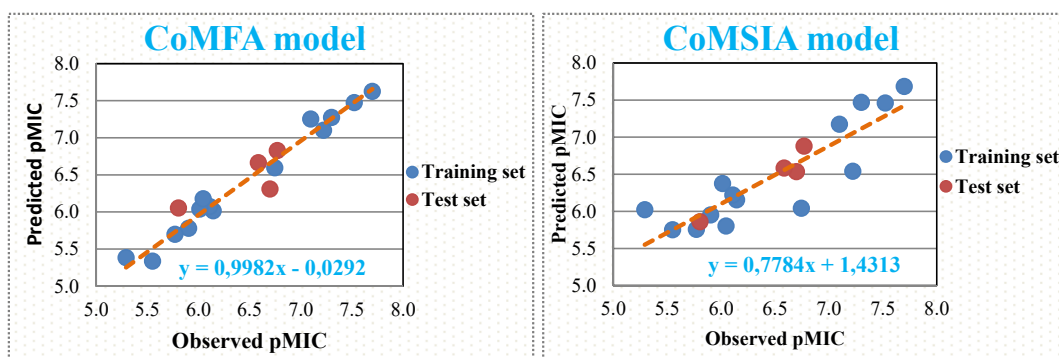

Figure 3. Plots of experimental and predicted pMIC values for the 18 carboxamides sulfonamide used in CoMFA and CoMSIA models.

between small molecule (ligand) and macromolecule (receptor) [35]. The 3D crystal of COVID-19 was extracted out of the Protein Data Bank (<http://www.rcsb.org>), (PDB code: **6LU7**) [36]. The all water molecules located in **6LU7** were wiped out and polar hydrogen atoms were appended for protein preparation. Discovery Studio 2016 [37] program was conducted to locate the active site of the concerned receptor (SAR-S-CoV-2 main protease). The original ligand of **6LU7** was removed; then, the most active molecule (compound **9**), the Chloroquine (CQ) and the proposed molecule (compound **P1**) were docked in the active site of COVID-19 receptor (PDB code: 6LU7), depending on Surflex-dock embedded in SYBYL-X 2.0 program. In this study, all ligands (molecule **9,** Chloroquine and proposed molecule **P1**) were minimized under the Tripos standard force field [28], using Gasteiger-Hückel charges by

conjugating gradient method with a gradient convergence criterion of 0.01 kcal/mol Å [29] in SYBYL software. Finally, to analyze the obtained outcomes, Discovery Studio 2016 [37] and PyMol's [38] software was applied.

2.8. ADMET prediction

ADMET properties are the most important technique employed to measure the properties and in silico pharmacokinetic parameters of the proposed molecules, thus, it affords a rapid and preliminary screening of ADMET properties before molecules are entirely examined in vitro because these newly molecules can be toxic or metabolized by the body. To that end, the pkCSM [39] and SwissADME [40] online tools are

Table 3. Experimental and predicted pMIC of 18 carboxamides sulfonamide derivatives and their residuals.

N°	pMIC	CoMFA		CoMSIA	
		Predicted	Residuals	Predicted	Residuals
1	6.143	6.017	0.126	6.156	-0.013
2	6.108	6.074	0.034	6.220	-0.112
3	7.523	7.474	0.049	7.460	0.063
4*	6.770	6.829	-0.059	6.879	-0.109
5	5.292	5.384	-0.092	6.022	-0.730
6	5.550	5.338	0.212	5.753	-0.203
7	6.745	6.596	0.149	6.043	0.702
8	7.097	7.253	-0.156	7.175	-0.078
9	7.699	7.625	0.074	7.684	0.015
10	7.222	7.102	0.120	6.541	0.681
11*	6.699	6.310	0.389	6.535	0.164
12*	5.804	6.054	-0.250	5.860	-0.056
13	6.013	6.039	-0.026	6.376	-0.363
14	6.046	6.178	-0.132	5.803	0.243
15	7.301	7.275	0.026	7.469	-0.168
16*	6.585	6.664	-0.079	6.584	0.001
17	5.903	5.781	0.122	5.953	-0.050
18	5.770	5.700	0.070	5.758	0.012

* Test set molecules.
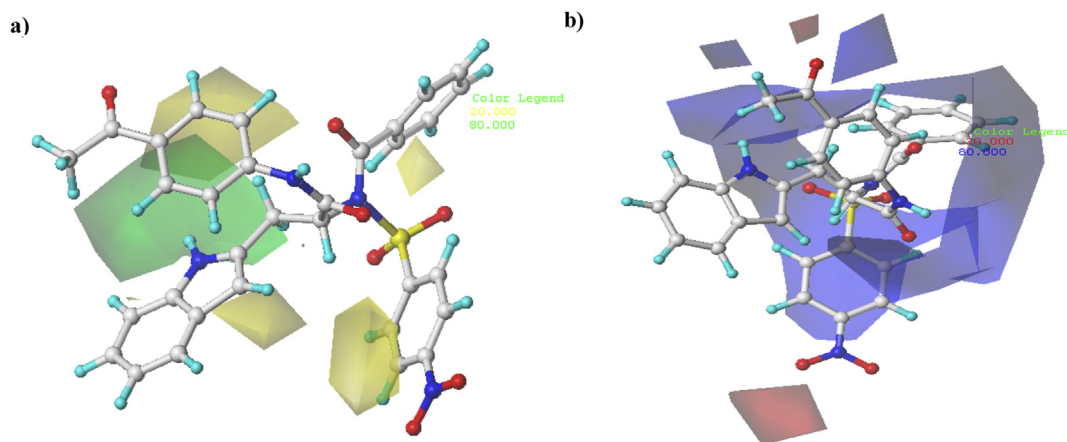
Figure 4. a) Steric and b) Electrostatic contours maps of CoMFA model using compound 9 as a reference.

adopted in order to predict the ADMET properties of eight proposed molecules.

3. Results and discussion

3.1. CoMFA and CoMSIA results

One of the aims of this study is to create trustworthy model that is why CoMFA and CoMSIA techniques were conducted and their statistical results were embodied in Table 2. Figure 3 clarifies the graphs of the experimental and predicted pMIC values for the 18 carboxamides sulfonamide analogs used in this study. Table 3 makes clear the observed and predicted pMIC values of 18 carboxamides sulfonamide analogs.

The outcomes of Table 2 point out that CoMFA and CoMSIA models have significant values of Q^2 (0.579 and 0.542 respectively), high values of R^2 (0.989 and 0.975 respectively), small standard error of the estimate SEE (0.097 and 0.148 respectively), and 4 as an optimum components (N). Further, the validation procedures are executed in order to determine the predictive stability of a model and to test the influence of each

sample (molecule) on the final model. External validation is one of them and is considered as an important step to verify the capabilities of the models. From Table 2, we notice that CoMFA and CoMSIA models have important values of R^2test (0.791 and 0.964 respectively) which are greater than 0.6; revealing that these models have high effectiveness. In a similar vein, electrostatic, steric, hydrophobic, acceptor and donor fields were made in order to determine the structural requirements which affect the activity. The excellent CoMFA model contains of two fields (steric and electrostatic), whilst the best CoMSIA model involves five fields: steric, electrostatic, hydrophobic, donor and acceptor contours. These findings make clear the excellent stability and the powerful predictive characteristics of the CoMFA and CoMSIA models.

According to Table 3, we notice that the residuals between predicted and experimental pMIC values are not more than 1 logarithm unit. Based on these observations, it seems that no compound in the series was regarded as an outlier.

The graphs presented in Figure 3 incarnate the good linear relationships. This illustrates that the bioactivities predicted by the derived models are in accordance with the experimental data; that is these models have powerful predictive capacity.
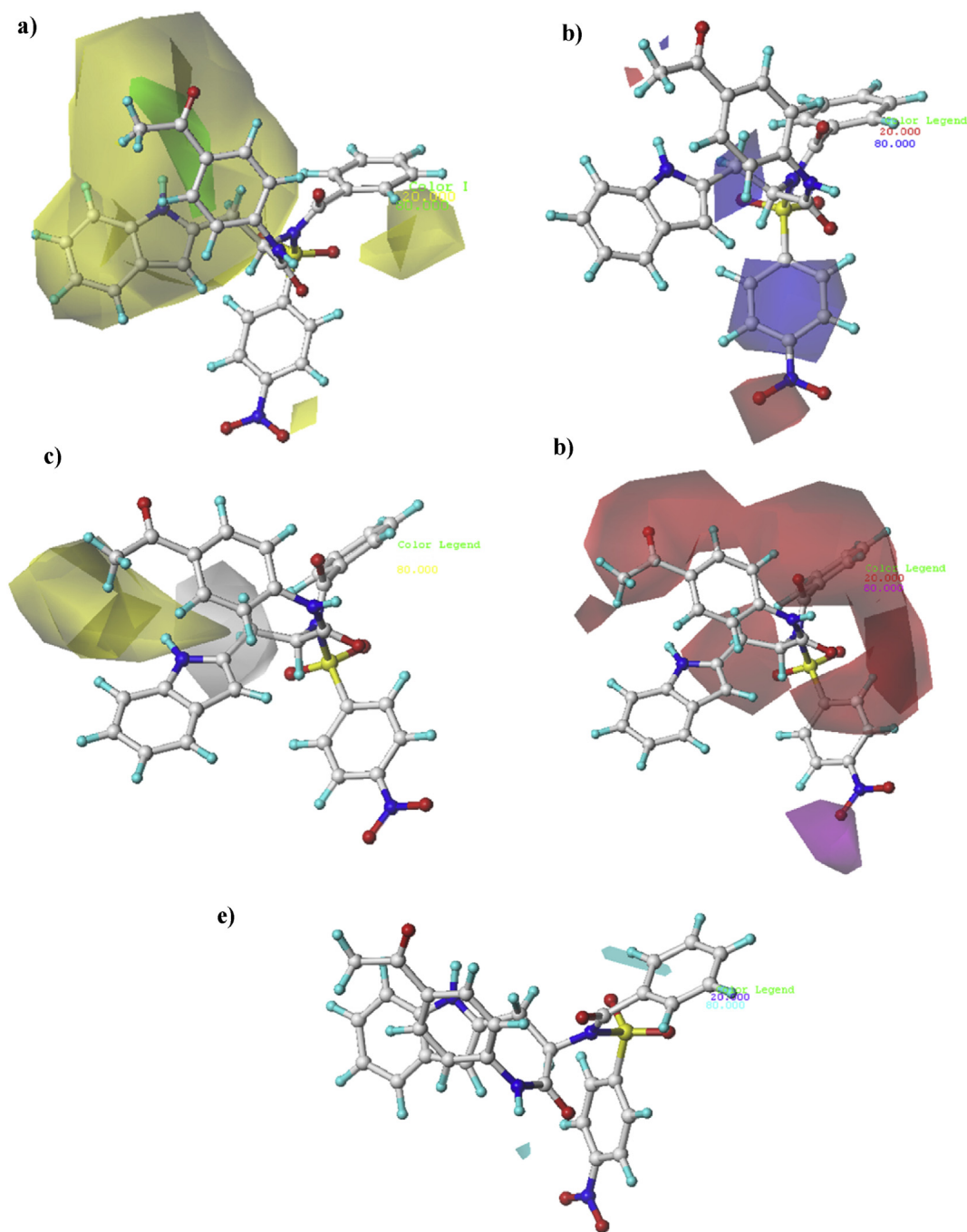
Figure 5. a) Steric, b) Electrostatic, c) Hydrophobic, d) H-bond donor and e) H-bond acceptor contours maps of CoMSIA analysis using compound 9 as a reference.

3.2. Graphical interpretation of CoMFA model

In order to visualize the information included in the good proposed CoMFA model, 3D-QSAR contour maps in three dimensional space were produced to identify the preferred and unpreferred moieties influencing the activity. The CoMFA steric and electrostatic contour maps are embodied in Figure 4. Compound **9** which is the most active molecule in the series; was adopted as reference structure to produce the CoMFA contour maps.

CoMFA steric contour maps depicted in Figure 4(a) make clear that green contour near the methyl group, which is nearby the 1H-indole group and the hydrogen atom of the same group, hints that huge groups in these positions could enhance the activity. On the other hand,

yellow contours surround the *meta* and *ortho* positions of the phenyl moiety, *ortho* and *meta* positions of the acetophenone group, and near the hydrogen atom which is located in position three of 1H-indole, point out that small groups in these positions might improve the activity. These results can explain the high activity of some compounds in the dataset, such as compound **3** (pMIC = 7.523) and compound **15** (pMIC = 7.301) which have tiny group in these places.

In the CoMFA electrostatic contour maps (Figure 5(b)), the red contour near the R_1 moiety exhibits that groups with electro-withdrawing character could improve the activity. On the other hand, the blue contours covering the sulfonamide group, around *ortho* and *meta* positions of the phenyl group, near oxygen atom of acetophenone group, and around hydrogen atom of 1H-indole show that substituents with electro-
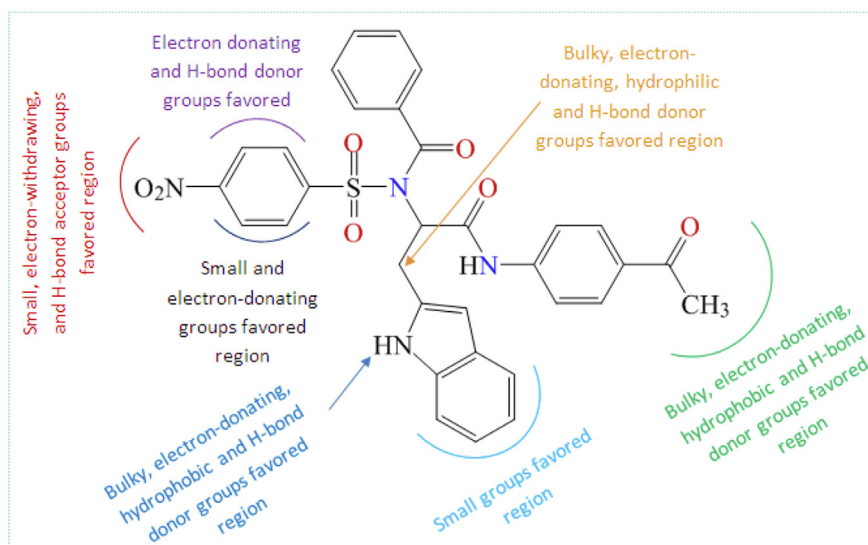
Figure 6. Summary of contour maps for antimalarial activity generated by CoMFA and CoMSIA models.

Table 4. Q^2 and R^2 values after several Y-randomization tests.

Iteration	CoMFA		CoMSIA	
	Q^2	R^2	Q^2	R^2
1	-0.089	0.945	-0.114	0.895
2	0.007	0.962	0.038	0.877
3	0.094	0.963	0.089	0.895
4	-0.018	0.956	-0.257	0.875
5	0.002	0.956	-0.266	0.872

donating character in these positions might increase the activity. Such findings will explain the important activity of the compound **10** (pMIC = 7.222) which has a moiety with electro-withdrawing nature in the R_1 position and a group with electro-donating nature in the R_2 position.

3.3. Graphical interpretation of CoMSIA model

In order to better understand the different fields that would impact (increasing or decreasing) the activity, CoMSIA contour maps including the hydrophobic, H-bond acceptor and H-bond donor fields as well as the steric and electrostatic fields were produced and their outcomes are clarified in Figure 5. Molecule **9** is the most active of the series; thus it was selected as a template to produce the CoMSIA contour maps.

As can be seen in Figure 5(a), a green contour near the methyl substituents which is nearby the 1H-indole moiety and the hydrogen atom of the same group make clear that huge groups in these positions can improve the activity. Instead, yellow contours near to the R_1 group, around the *ortho* position of the phenyl moiety and covering the R_2 group, make clear that these regions are reserved only for tiny moiety to enhance the activity.

In the CoMSIA electrostatic contour maps (Figure 5(b)), the red contour around the R_1 moiety point out that group with electro-withdrawing character could ameliorate the activity. Instead, the blue contours cover phenyl of the sulfonamide moiety, and around methyl group which is near 1H-indole moiety, make clear that substituents with electro-withdrawing character in these positions might be helpful for the activity.

In the CoMSIA hydrophobic contour maps (Figure 5(c)), a yellow contour is seen near the hydrogen atom of the 1H-indole groups hints that moiety with hydrophobic character at this position could be helpful for enhancing the potency. Instead, a white contour cover methyl group

which is near to 1H-indole group hints that the addition of hydrophilic groups in this position might improve the potency.

The magenta contour near the R1 moiety hints that this region is reserved only for the moiety with hydrogen bond acceptor character to develop the activity (Figure 5(d)). Instead, the red contours around acetone, *ortho* and *meta* positions of acetophenone group, cover *ortho* and *meta* positions of sulfonamide moiety and around methyl moiety which is near to 1H-indole group, make clear that groups with hydrogen bond acceptor character could decrease the activity ((Figure 5(d)).

The tiny cyan contour around the *ortho* position of the phenyl group hints that substituents with hydrogen bond donor character could enhance the activity (Figure 5(e)).

In Figure 6, we abstracted all information extracted from CoMFA and CoMSIA contour maps results, which could be much useful to scrutinize the structural requirements that influence the activity and consequently propose new potent carboxamides sulfonamide derivatives with important inhibitory activity.
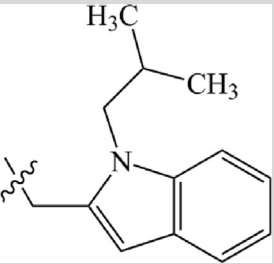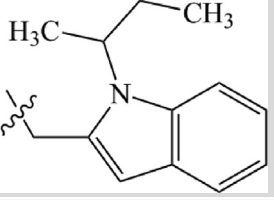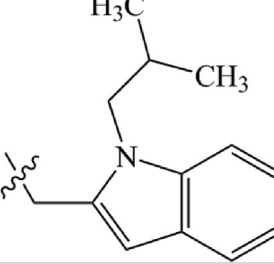
3.4. Y-randomization
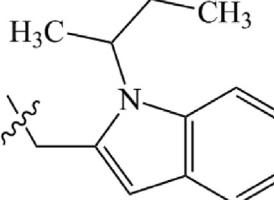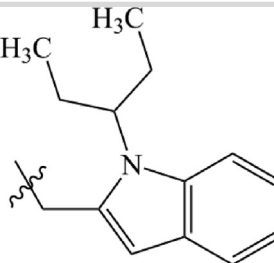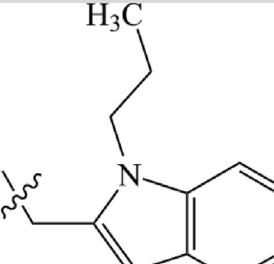
In the aim to scrutinize and test the capacity of the molded model, the Y-randomization technique was executed. Results of Table 4 display that CoMFA and CoMSIA models after this validation have lower values of Q^2 and R^2 compared to our original models, which proves that these models have powerful capability.

3.5. Design of new molecules

The main goal of this study is to design new potent inhibitors against COVID-19, for that, the all information extracted from CoMFA and CoMSIA contour maps outcomes guided us to identify the structural
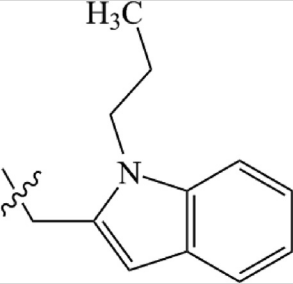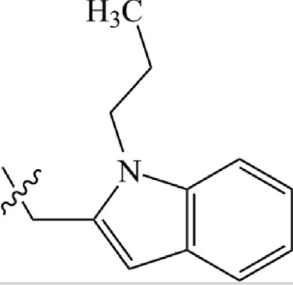
Table 5. Chemical structures of newly designed compounds and their predicted pMIC based on CoMFA and CoMSIA models.

N°	Structure			Predicted pMIC	
	R₁	R₂		CoMFA	CoMSIA
P1	CN			7.856	8.382
P2	CN			7.753	8.492
P3	NO			7.673	8.571
P4	NO			7.528	8.373
P5	NO			7.530	8.361
P6	NO			7.477	8.333

Table 5 (*continued*)

N°	Structure		Predicted pMIC	
	R₁	R₂	CoMFA	CoMSIA
P7	CN	H₃C (structure)	7.661	8.033
P8	NO₂	H₃C (structure)	7.844	7.973

Figure 7. The interaction modes of the more potent molecule (compound **9**) and COVID-19 main protease.

Figure 8. The blind docked conformations of Chloroquine in the active site of COVID-19 main protease.

requirements that influence the activity. Therefore, 8 carboxamides sulfonamide derivatives were proposed and designed with important activities compared to the molecule **9** (The more active molecule in dataset). These molecules were minimized and aligned to the database using molecule **9** as a template and their theoretical pMI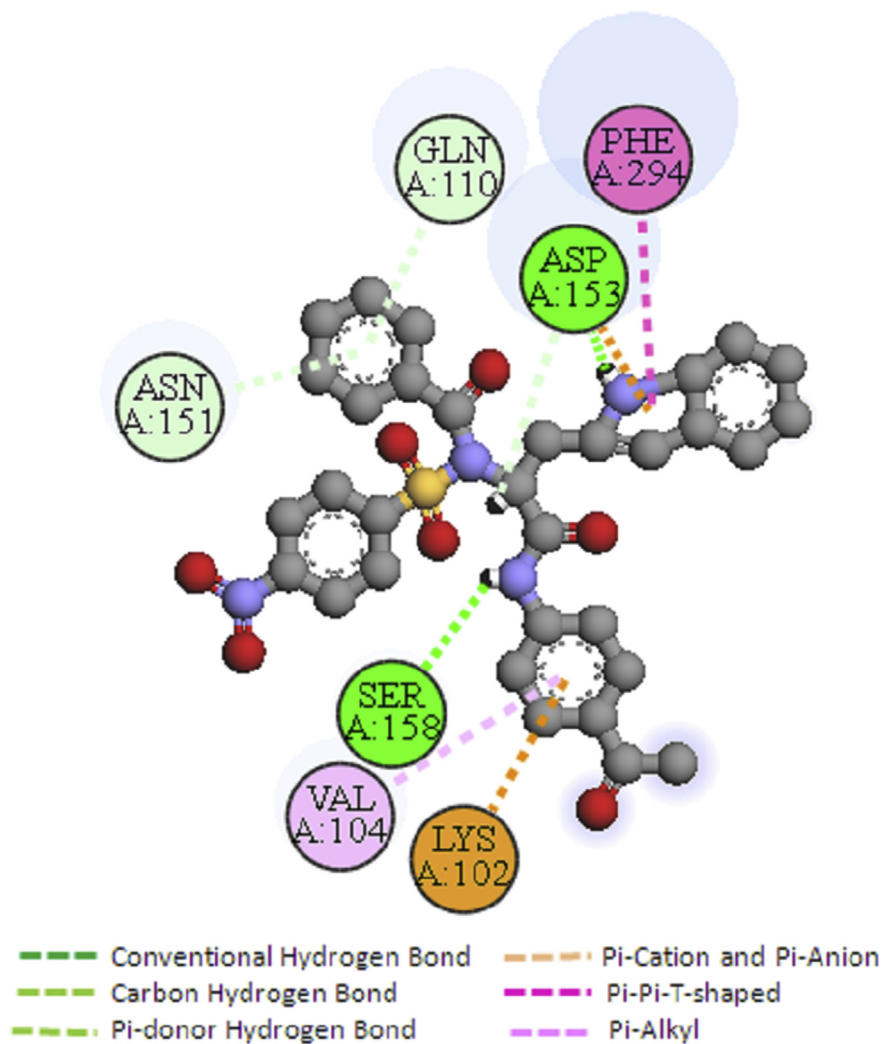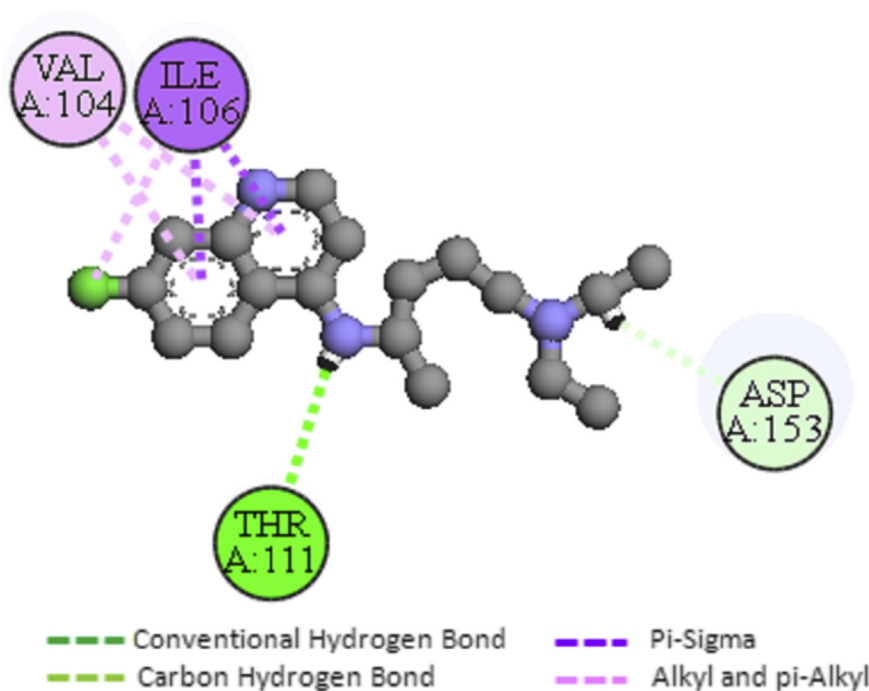C values were predicted using the proposed CoMFA and CoMSIA models. The predicted pMIC of the 8 carboxamides sulfonamide scaffolds and their chemical structures are embodied in Table 5.

3.6. Docking results

Chloroquine is an antimalarial drug that has demonstrated inhibition activity on coronavirus replication in vitro [6,7,8]. In the aim to develop new drug that may be more potent than Chloroquine against SARS-CoV-2; we executed surflex-docking on compound **9**, Chloroquine and the proposed molecule **P1** with SARS-CoV-2 receptor PDB: 6LU7.

Figure 7 makes clear the binding mode of the molecule **9** which is the most active compound in the series. This molecule affords numerous interactions with COVID-19 main protease, such as pi-donor hydrogen bond interaction with ASN 151 and GLN 110 residues, pi-cation, and pi-anion interactions with LYS 102 and ASP A: 153 residues. Additionally, the 1H-indole group provides a conventional hydrogen bond and pi-pi-T-shaped interactions with PHE 294 and ASP 153 residues, respectively. The group (-NH) which is near acetophenone moiety also forms a conventional hydrogen bond interaction with SER 158 residue. Likewise, compound **9** affords also a pi-alkyl interaction with VAL 104 residue. These outcomes reveal that the compound 9 has high stability in the active site of the receptor.

The interaction results of the Chloroquine and COVID-19 main protease (Figure 8) provides carbon-hydrogen bond interaction with ASP 153 residue and conventional hydrogen bond interaction with THR 111 residue; similarly, the 7-chloroquinoline moiety affords an alkyl, pi-alkyl, and pi-sigma interactions with VAL 104 and ILE 106 residues, respectively.

Continuously, the proposed compound **P1** provides several types of interactions with COVID-19 main protease (Figure 9) such as, pi-alkyl interactions with PHE 8, ILE 249, ILE 106, PHE 294, VAL 297 residues, and pi-anion interaction with ASP 153 residue. Additionally, the

acetophenone ring offers pi-anion and pi-pi-T-shaped interactions with ASP 153 and PHE 294 residues, respectively. In a similar vein, the oxygen atom of sulfur dioxide group presents a conventional hydrogen bond interaction with PHE 294 residue. All these interactions make clear the high stability of the proposed compound **P1** in the active site of COVID-19 main protease. In Figure 10, the magenta color around R groups denotes that this region is reserved only for the groups with hydrogen bond donor character, on the other hand, the green color around R group displays that this region is beneficial for the substituents with hydrogen bond acceptor character. Moreover, the blue color around R position exhibits that groups with hydrophobic character are unfavored in this region, while the brown color clarifies the regions preferred by the hydrophobic groups.

The outcomes of Table 6 hint that the proposed compound **P1** has a high binding affinity (total scoring) than compound **9** and Chloroquine, which implies that our candidate scaffold **P1** has a good binding affinity and high stability in the active site of COVID-19 main protease compared to the molecule **9** and the Chloroquine (CQ).

3.7. Docking validation protocol

In order to validate and check the efficiency of the docking procedure, a re-docking of the co-crystallized ligand was executed. The superposition between the co-crystalized ligand N3 and the docked ligand conformation was exposed in Figure 11.

Figure 11 shows that the co-crystalized ligand N3 bound almost in a comparable position compared to that observed for the docked ligand conformation. These outcomes underline that molecular docking simulation was effectively verified.

As observed in Figure 12, the co-crystallized ligand (inhibitor N3) affords numerous interactions with COVID-19 main protease, like alkyl and pi-alkyl interactions with MET 49, HIS 41, CYS 145 and HIS 163 residues. The inhibitor N3 also forms pi-sigma interactions with GLY 143 and THR 25 residues and three conventional hydrogen bond interactions with PHE 140, THR 26 and THR 24 residues. In a similar vein, the ligand N3 offers carbon hydrogen bond interactions with GLU 166, THR 25 and ASN 142 residue. These outcomes hint the suggested molecule P1 will be an efficient inhibitors for COVID-19.
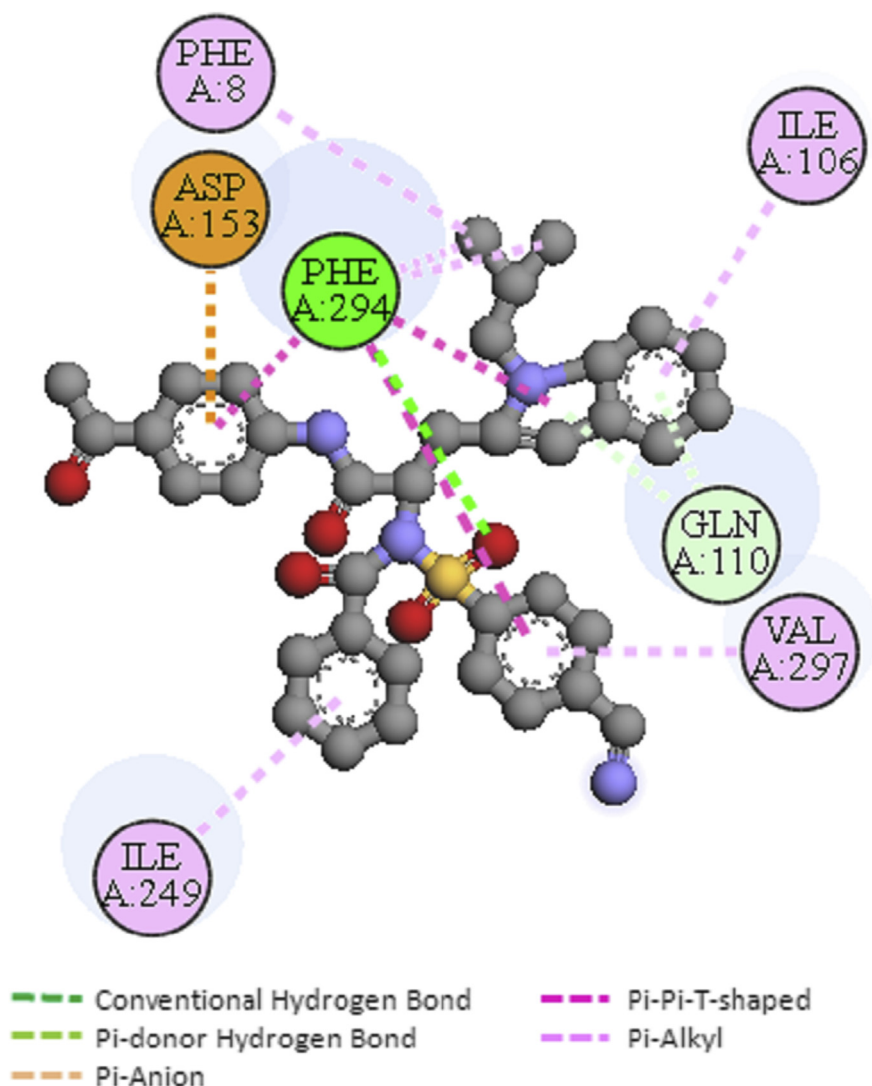
Figure 9. Docking interactions between the proposed compound **P1** and COVID-19 main protease.

3.8. ADMET results

The discovery of a drug is a crucial step but it remains insufficient because this drug can exhibit its limitations; it can be toxic or can have poor ADMET properties. For this reason, the prediction of ADMET properties regarded as an essential step to decrease potential challenges later throughout clinical treatments. Thence, pkCSM [39] and SwissADME [40] are online tools adopted to predict the ADMET properties of the new carboxamides sulfonamide derivatives.

The blood-brain barrier (BBB) is the main interface separating the central nervous system (CNS) and the blood circulation (BC); it's a significant property since it controls if drugs can pass BBB or not and also exerts its effect on the brain [41]. A molecule with logBB > -1 considered highly distributed to the brain. Consequently, the results of BBB permeability in Table 7 make clear non-penetrating BBB for new proposed molecules. Moreover, water solubility is given in log (mol/L) (Insoluble < -10 < poorly < -6 < Moderately < -4 <Soluble < -2 < Very soluble <0 < highly soluble), results of Table 7 indicate that all newly carboxamides sulfonamide are soluble.

A compound with intestinal absorbance value greater than 30% is considered to be highly absorbed; showing that the 8 carboxamides sulfonamide are absorbed by the human intestine. Moreover, concerning the Caco-2 permeability, the outcomes of Table 7 point out that the 8 newly carboxamides sulfonamide derivatives cannot penetrate to Caco-2

(high permeability would translate in a predicted value larger than 0.9). Additionally, all suggested molecules demonstrated to be a potential substrate for P-glycoprotein substrate and inhibitor which effluxes drugs and many compounds to subject further clearance and metabolism [42]. In fact, the inhibition of cytochrome P450 isoforms can cause drug-drug interactions in which co-administered drugs fail to be metabolized and accumulate to toxic levels [43]. However, the 8 carboxamides sulfonamide scaffolds could be inhibiting some of the cytochrome P450 isoforms. Moreover, the safety of the molecules is an important parameter to develop a successful drug; for this, the compound-induced toxicity was predicted for Ames test using in silico tools [44]. As shown in Table 7, results specify that all newly designed molecules were non-mutagenic, respecting Ames test data.

The outcomes of in silico ADMET parameters point out that the proposed scaffolds revealed a clear advantage in terms of BBB, Caco-2 permeability, intestinal adsorption and toxicity; consequently, it can be presumed that all newly carboxamides sulfonamides present good biological activity, drug-like characteristics and in silico ADMET properties.

4. Conclusion

In the aim of discovering new potent drugs against COVID-19, the 3D-QSAR and molecular docking studies were applied on a series of eighteen carboxamides sulfonamide derivatives. The optimal CoMFA and CoMSIA
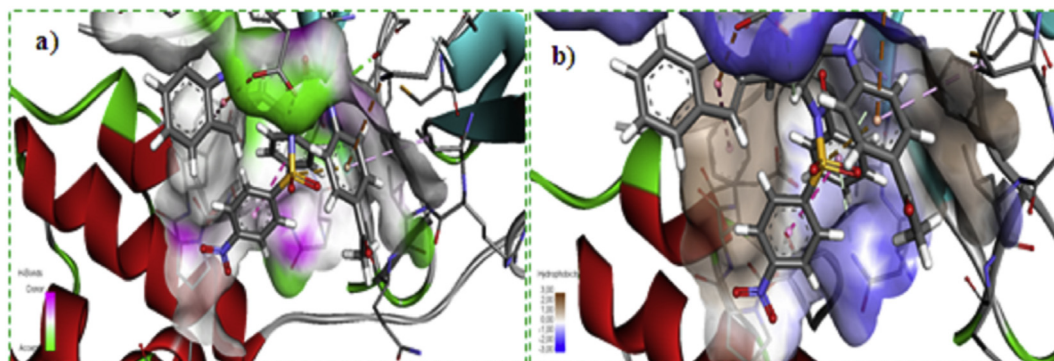
Figure 10. 3D View of the binding conformation of the compound **9** at the active site of COVID-19 main protease (Hydrogen Bond (**a**) and hydrophobicity (**b**) interactions).

Table 6. Docking interactions and total scoring of compound **9**, Chloroquine and **P1** with **6LU7** receptor.

Compounds	Residues	Scoring
Compound **9**	Asp 153, Ser 158, Gln 110, Asn 151, Val 104, Lys 102, Phe 294	4.11
Chloroquine	Thr 111, Asp 153, Val 104, Ile 106	3.51
P1	Phe 294, Gln 110, Phe 8, Ile 106, Val 297, Ile 249, Asp 153	4.46
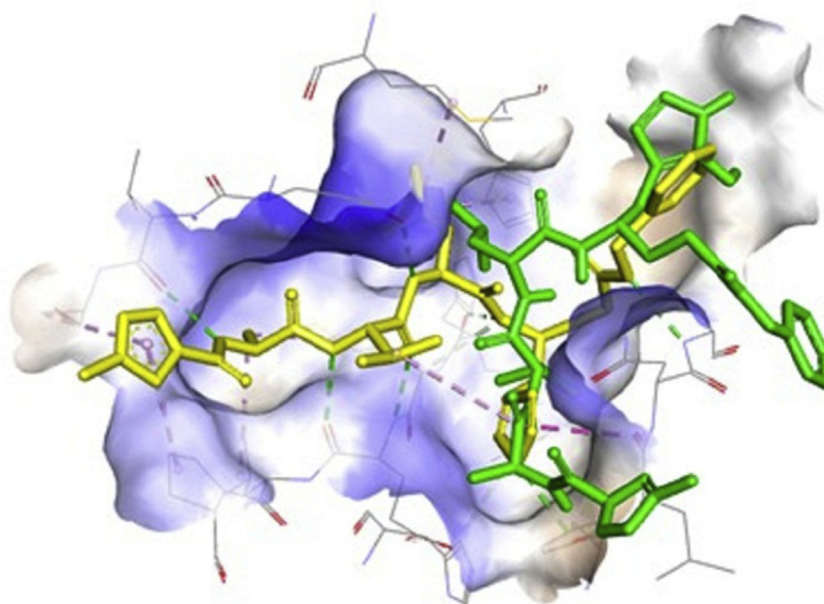
Figure 11. Superimposing of default conformation (Yellow colored) on docked conformation (Green colored) of the co-crystallized ligand N3 validating docking simulation.

models disclosed good statistical outcomes in terms of several rigorous statistical keys, such as Q^2, R^2 and R^2test, thence, these models can be capably espoused to predict new scaffolds with important activity. The contour maps produced by CoMFA and CoMSIA models, reveal the important sites where steric, electrostatic, and hydrophobic interactions might significantly influencing (increase or decrease) the activity of the molecules. These contour maps guided us to propose eight molecules with important inhibitory activity. The molecular surflex-docking between molecule **9** (the most active molecule), CQ, the proposed compound **P1** and the crystal structure of SARS-CoV-2 main protease (PDB code 6LU7) displayed that molecule **P1** has a good binding affinity and high stability in the active site of the studied protein. Indeed, ADMET outcomes of the predicted carboxamides sulfonamide scaffolds are depicted good pharmacokinetic properties with the acceptable absorption, good metabolism transformation, and are found to be neither toxic, which can be granted as reliable inhibitors for SARS-CoV-2.

Declarations

Author contribution statement

Ayoub Khaldan: Analyzed and interpreted the data; Wrote the paper.

Soukaina Bouamrane, Fatima En-Nahli, Reda El-mernissi, Khalil El khatabi, Rachid Hmamouchi: Analyzed and interpreted the data.

Hamid Maghat, Abdelouahid Sbai, Tahar Lakhlifi: Conceived and designed the experiments.
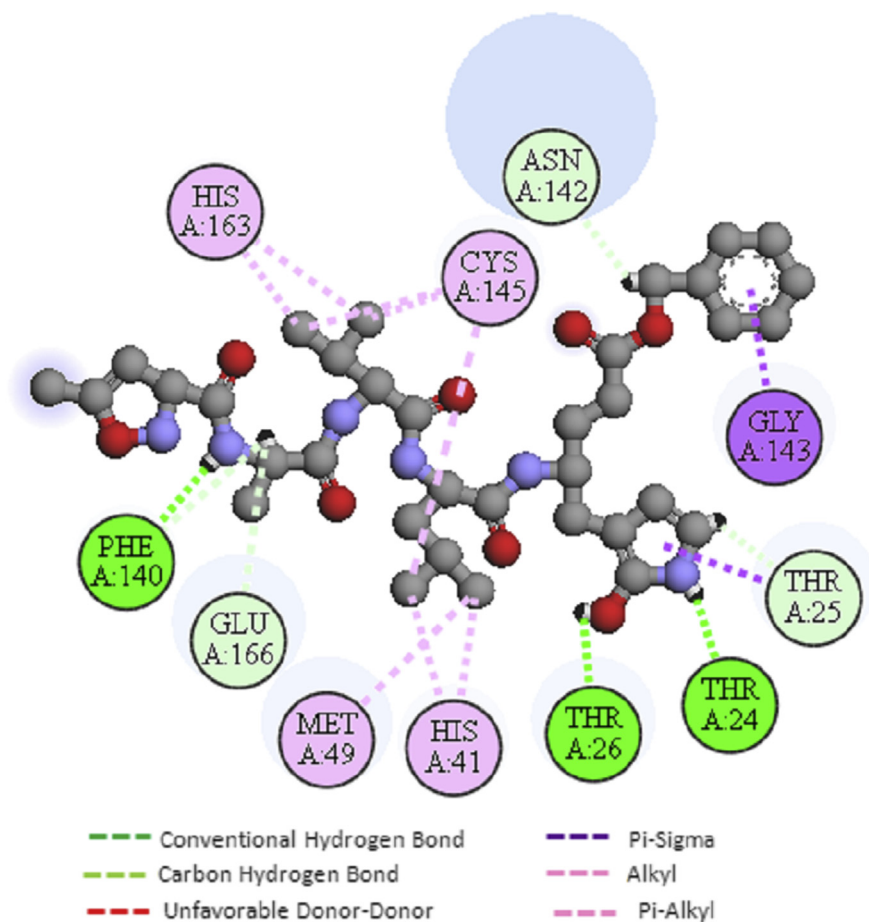
Figure 12. The Blind Docked conformations of inhibitor **N3** (co-crystallized ligand) and SARS-CoV-2 protein.

Table 7. In silico ADMET prediction and synthetic accessibility values of the new 8 carboxamides sulfonamide derivatives.

Models		Compounds							
		P1	P2	P3	P4	P5	P6	P7	P8
Absorption (A)									
Water solubility	Numeric (Log mol/L)	-3.87	-3.98	-3.84	-3.94	-3.87	-3.93	-3.96	-3.48
Caco-2 permeability	Numeric (log Papp in 10^{-6} cm/s)	0.90	0.83	0.84	0.77	0.74	0.83	0.89	0.08
Intestinal absorption (human)	Numeric (% Absorbed)	90.09	91.49	92.49	93.89	94.51	92.37	89.97	89.58
P-glycoprotein substrate	Categorical (Yes/No)	No	No	No	No	No	No	No	No
P-glycoprotein inhibitor		Yes	Yes	Yes	Yes	Yes	Yes	Yes	Yes
Distribution (D)									
Blood-brain barrier (logBB)	Numeric (log BB)	-0.65	-1.09	-0.86	-0.85	-0.84	-0.88	-0.67	-1.00
Metabolism (M)									
CYP1A2 inhibitor	Categorical (Yes/No)	No	No	No	No	No	No	No	No
CYP2C9 inhibitor		Yes	Yes	Yes	Yes	Yes	Yes	Yes	Yes
CYP2D6 inhibitor		No	No	No	No	No	No	No	No
CYP2C19 inhibitor		Yes	Yes	Yes	Yes	Yes	Yes	Yes	Yes
CYP3A4 inhibitor		Yes	Yes	Yes	Yes	Yes	Yes	Yes	Yes
CYP2D6 substrate		No	No	No	No	No	No	No	No
CYP3A4 substrate		Yes	Yes	Yes	Yes	Yes	Yes	Yes	Yes
Excretion (E)									
Total Clearance	Numeric (log ml/min/kg)	-0.09	0.01	-0.18	-0.07	-0.01	-0.01	0.07	-0.003
Toxicity (T)									
AMES toxicity	Categorical (Yes/No)	No	No	No	No	No	No	No	No
Synthetic accessibility	Numeric	4.92	5.19	4.89	5.15	5.01	4.77	4.80	4.82

References

[1] C. Huang, Y. Wang, X. Li, L. Ren, et al., Clinical features of patients infected with 2019 novel coronavirus in Wuhan, China, Lancet 395 (2020) 497–506.

[2] R. Lu, X. Zhao, J. Li, P. Niu, et al., Genomic characterisation and epidemiology of 2019 novel coronavirus: implications for virus origins and receptor binding, Lancet 395 (2020) 565–574.

[3] N. Zhu, D. Zhang, W. Wang, X. Li, et al., A novel coronavirus from patients with pneumonia in China, N. Engl. J. Med. 382 (2020) 727–733.

[4] World Health Organization, Coronavirus disease (COVID-19) outbreak. https://www.who.int.

[5] K. Ma, Y. Zhang, T. Hou, M. Wu, W. Cai, T. Wen, Investigation of physical and mental health in isolated people during the outbreak of Novel Coronavirus Pneumonia, Chin. J. Clin. Med. 27 (2020) 36–40.

[6] J. Gao, Z. Tian, X. Yang, Breakthrough: chloroquine phosphate has shown apparent efficacy in treatment of COVID-19 associated pneumonia in clinical studies, BioSci. Trends. 14 (2020) 72–73.

[7] P. Gautret, J.-C. Lagier, P. Parola, V.T. Hoang, L. Meddeb, M. Mailhe, et al., Hydroxychloroquine and azithromycin as a treatment of COVID-19: results of an open-label non-randomized clinical trial, Int. J. Antimicrob. Agents 56 (2020) 105949.

[8] C.A. Devaux, J.-M. Rolain, P. Colson, D. Raoult, New insights on the antiviral effects of chloroquine against coronavirus: what to expect for COVID-19? Int. J. Antimicrob. Agents 55 (2020) 105938.

[9] R. Yu, L. Chen, R. Lan, R. Shen, P. Li, Computational screening of antagonist against the SARS-CoV-2 (COVID-19) coronavirus by molecular docking, Int. J. Antimicrob. Agents 56 (2020) 106012.

[10] T.V. Wani, S. Bua, P.S. Khude, A.H. Chowdhary, C.T. Supuran, M.P. Toraskar, Evaluation of sulphonamide derivatives acting as inhibitors of human carbonic anhydrase isoforms I, II and Mycobacterium tuberculosis β-class enzyme Rv3273, J. Enzym. Inhib. Med. Chem. 33 (2018) 962–971.

[11] A.A.E. Kools, J.F. Moltmann, T. Knacker, Estimatimating the use of veterinary medicines in the European Union, Regul. Toxicol. Pharmacol. 50 (2008) 59–65.

[12] S.S. Swain, S.K. Paidesetty, R.N. Padhy, Antibacterial activity, computational analysis and host toxicity study of Thymol-sulfonamide conjugates, Biomed. Pharmacother. 88 (2017) 181–193.

[13] T. Han, M. Goralski, N. Gaskill, E. Capota, J. Kim, T.C. Ting, Y. Xie, N.S. Williams, D. Nijhawan, Anticancer sulfonamides target splicing by inducing RBM39 degradation via recruitment to DCAF15, Science 356 (2017), eaal7977, 6336.

[14] M.M. Ghorab, F.A. Ragab, H.I. Heiba, A.M. Soliman, Design and synthesis of some novel 4-chloro-N-(4-(1-(2-(2-cyanoacetyl)hydrazono)ethyl)phenyl) benzenesulfonamide derivatives as anticancer and radiosensitizing agents, Eur. J. Med. Chem. 117 (2016) 8–18.

[15] V. Gorantla, R. Gundla, S.S. Jadav, S.R. Anugu, J. Chimakurthy, S.K. Nidasanametla, R. Korupolu, Molecular hybrid design, synthesis and biological evaluation of N-phenyl sulfonamide linked N-acyl hydrazone derivatives functioning as COX-2 inhibitors: new anti-inflammatory, anti-oxidant and anti-bacterial agents, New J. Chem. 41 (2017) 13516–13532.

[16] A. Nocentini, C.T. Supuran, Carbonic anhydrase inhibitors as antitumor/antimetastatic agents: a patent review (2008-2018), Expert Opin. Ther. Pat. 28 (2018) 729–740.

[17] K.M. Parai, G. Panda, K. Srivastava, P.S. Kumar, Design, synthesis and antimalarial activity of benzene and isoquinoline sulfonamide derivatives, Bioorg. Med. Chem. Lett 18 (2008) 776–781.

[18] J.N. Dominguez, C. Leon, J. Rodrigues, N.G. de Dominguez, J. Gut, P.J. Rosenthal, Synthesis and antimalarial activity of sulfonamide chalcone derivatives, Il Farmaco 60 (2005) 307–331.

[19] B. Nubia, C.S.P. Luiz, A.S. Osvaldo, C.S. Isabor, Design and synthesis of new N-(5-Trifluoromethyl)-1H-1,2,4-triazol-3-yl benzenesulfonamides as possible antimalarial prototypes, Molecules 16 (2011) 8083–8097.

[20] A. Khaldan, K. El khatabi, R. El-mernissi, A. Sbai, M. Bouachrine, T. Lakhlifi, Combined 3D-QSAR modeling and molecular docking study on metronidazole-triazole-styryl hybrids as antiamoebic activity, Moroc. J. Chem. 8 (2020) 527–539.

[21] S. Pirhadi, J.B. Ghasemi, 3D-QSAR analysis of human immunodeficiency virus entry-1 inhibitors by CoMFA and CoMSIA, Eur. J. Med. Chem. 45 (2010) 4897–4903.

[22] A.N. Jain, Surflex: fully automatic flexible molecular docking using a molecular similarity-based search engine, J. Med. Chem. 46 (2003) 499–511.

[23] J. Wang, P.A. Kollman, I.D. Kuntz, Flexible ligand docking: a multistep strategy approach, Proteins 36 (1999) 1–19.

[24] D.I. Ugwu, U.C. Okoro, P.O. Ukoha, S. Okafor, A. Ibezim, N.M. Kumar, Synthesis, characterization, molecular docking and in vitro antimalarial properties of new carboxamides bearing sulfonamide, Eur. J. Med. Chem. 135 (2017) 349–369.

[25] R.D. Cramer, D.E. Patterson, J.D. Bunce, Comparative molecular field analysis (CoMFA). 1. Effect of shape on binding of steroids to carrier proteins, J. Am. Chem. Soc. 110 (1988) 5959–5967.

[26] G. Klebe, U. Abraham, T. Mietzner, Molecular similarity indices in a comparative analysis (CoMSIA) of drug molecules to correlate and predict their biological activity, J. Med. Chem. 37 (1994) 4130–4146.

[27] Sybyl 8.1; Tripos Inc.: St. Louis, MO, USA, 2008; Available online: http://www.tripos.com (accessed on 26 January 2011)

[28] M. Clark, R.D. Cramer, N. Van Opdenbosch N, Validation of the general purpose tripos 5.2 force field, J. Comput. Chem. 10 (1989) 982–1012.

[29] W.P. Purcell, J.A. Singer, A brief review and table of semiempirical parameters used in the Hueckel molecular orbital method, J. Chem. Eng. Data 12 (1967) 235–246.

[30] A. Belhassan, S. Chtita, T. Lakhlifi, M. Bouachrine, 3D-QSPR studies of olfactive property for pyrazine derivatives, Proceedings BIOSUNE'1 – (2018) 1–7, 2018.

[31] L. Ståhle, S. Wold, Multivariate data analysis and experimental design in biomedical research, Prog. Med. Chem. 25 (1988) 291–338.

[32] B.L. Bush, R.B. Nachbar, Sample-distance partial least squares: PLS optimized for many variables, with application to CoMFA, J. Comput. Aided Mol. Des. 7 (1993) 587–619.

[33] A. Golbraikh, A. Tropsha, Beware of q2!, J. Mol. Graph. Model. 20 (2002) 269–276.

[34] C. Rücker, G. Rücker, M. Meringer, Y-randomization and its variants in QSPR/QSAR, J. Chem. Inf. Model. 47 (2007) 2345–2357.

[35] A. Khaldan, R. El-Mernissi1, A. Ghaleb, R. Hmamouchi, A. Sbai1, M. Bouachrine, T. Lakhlifi, 3D-QSAR Modeling and Molecular Docking Studies of novel triazoles-quinine derivatives as antimalarial agents, J. Mater. Environ. Sci. 11 (2020) 429–443.

[36] X. Liu, B. Zhang, Z. Jin, H. Yang, Z. Rao, The crystal structure of COVID-19 main protease in complex with an inhibitor N3, Nature 582 (2020) 289–293.

[37] Dassault Systèmes BIOVIA, Discovery Studio Modeling Environment, Release 2017, Dassault Systèmes, San Diego, 2016 [WWW document], http://accelrys.com/products/collaborativescience/biovia-discovery-studio/. (Accessed 25 February 2017).

[38] W. DeLano, The PyMOL Molecular Graphics System DeLano Scientific, Palo Alto, CA, USA, 2002. http://www.pymol.org. (Accessed 25 February 2017).

[39] D.E.V. Pires, T.L. Blundell, D.B. Ascher, pkCSM: predicting small-molecule pharmacokinetic and toxicity properties using graph-based signatures, J. Med. Chem. 58 (2015) 4066–4072.

[40] A. Daina, O. Michielin, V. Zoete, SwissADME: a free web tool to evaluate pharmacokinetics, drug-likeness and medicinal chemistry friendliness of small molecules, Sci. Rep. 7 (2017) 42717.

[41] R.K. Upadhyay, Drug delivery systems, CNS protection, and the blood brain barrier, BioMed Res. Int. (2014) 1–37.

[42] M.L. Amin, P-glycoprotein inhibition for optimal drug delivery, Drug Target Insights 7 (2013) 27–34.

[43] T. Lynch, A. Price, The effect of cytochrome P450 metabolism on drug response, interactions, and adverse effects, Am. Fam. Physician 76 (2007) 391–396.

[44] H. Hadni, M. Elhallaoui, 3D-QSAR, docking and ADMET properties of aurone analogues as antimalarial agents, Heliyon 6 (2020), e03580.